

# Elf3 drives $\beta$ -catenin transactivation and associates with poor prognosis in colorectal cancer

J-L Wang<sup>1,3</sup>, Z-F Chen<sup>1,3</sup>, H-M Chen<sup>1,3</sup>, M-Y Wang<sup>1</sup>, X Kong<sup>1</sup>, Y-C Wang<sup>1</sup>, T-T Sun<sup>1</sup>, J Hong<sup>1</sup>, W Zou<sup>2</sup>, J Xu<sup>\*1</sup> and J-Y Fang<sup>\*1</sup>

Aberrant regulation of the Wnt/ $\beta$ -catenin pathway plays important roles in colorectal carcinogenesis, with over 90% of cases of sporadic colon cancer featuring  $\beta$ -catenin accumulation. While ubiquitination-mediated degradation is widely accepted as a major route for  $\beta$ -catenin protein turnover, little is known about the regulation of  $\beta$ -catenin in transcriptional level. Here we show that Elf3, a member of the E-twenty-six family of transcription factors, drives  $\beta$ -catenin transactivation and associates with poor survival of colorectal cancer (CRC) patients. We first found recurrent amplification and upregulation of Elf3 in CRC tissues, and further Gene Set Enrichment Analysis identified significant association between Elf3 expression and activity of WNT/ $\beta$ -catenin pathway. Chromatin immunoprecipitation and electrophoretic mobility shift assay consistently revealed that Elf3 binds to and transactivates  $\beta$ -catenin promoter. Ectopic expression of Elf3 induces accumulation of  $\beta$ -catenin in both nucleus and cytoplasm, causing subsequent upregulation of several effector genes including c-Myc, VEGF, CCND1, MMP-7 and c-Jun. Suppressing Elf3 in CRC cells attenuates  $\beta$ -catenin signaling and decreases cell proliferation, migration and survival. Targeting Elf3 in xenograft tumors suppressed tumor progression *in vivo*. Taken together, our data identify Elf3 as a pivotal driver for  $\beta$ -catenin signaling in CRC, and highlight potential prognostic and therapeutic significance of Elf3 in CRC.

*Cell Death and Disease* (2014) 5, e1263; doi:10.1038/cddis.2014.206; published online 29 May 2014

**Subject Category:** Cancer

Colorectal cancer (CRC) is the second most commonly diagnosed cancer in females and the third in males, with over 1.2 million new cancer cases and 600 000 deaths every year.<sup>1–3</sup> The development of CRC involves stepwise accumulation of somatic genetic alterations,<sup>4</sup> starting with inactivation of the tumor suppressor gene adenomatous polyposis coli (APC) or activation of the oncogene  $\beta$ -catenin (CTNNB1).<sup>5</sup> Accumulation of  $\beta$ -catenin, which leads to enhanced TCF/LEF-1 driven transcription and thereby contributes to tumor development,<sup>6,7</sup> can result from mutation of  $\beta$ -catenin itself or Wnt pathway inhibition of the GSK-3 $\beta$  kinase that together with APC promotes  $\beta$ -catenin degradation.<sup>8</sup> Nevertheless, emerging evidence shows that the activation of  $\beta$ -catenin can occur independently of Wnt signaling to GSK-3 $\beta$ .<sup>9,10</sup> Bz2 has also been found to induce Wnt-independent activation of  $\beta$ -catenin pathway,<sup>11</sup> and tumor cells overexpressing EGF receptor display GSK-3 $\beta$ -independent activation of  $\beta$ -catenin,<sup>12</sup> which is mediated by the embryonic pyruvate kinase M2.<sup>13</sup> Despite these findings, it remains unclear if other Wnt-independent mechanisms might be involved in  $\beta$ -catenin activation during CRC development.

Here we show that Elf3, a member of the E-twenty-six (Ets) family of transcription factors,<sup>14–16</sup> drives Wnt-independent  $\beta$ -catenin transactivation in CRC and associates with

poor patient survival. Previous studies showed that Elf3 inactivation leads to fetal death and defective terminal differentiation of enterocytes in the small intestine, but the role of Elf3 in CRC is currently unknown. We found that Elf3 gene is recurrently amplified in the genome of CRC, and Elf3 mRNA and protein levels are significantly unregulated in CRC tissues. Elf3 expression is required for the maintenance of proliferative and invasive phenotypes of CRC cells, and Gene Set Enrichment analysis (GSEA) revealed significant association between Elf3 and activity of the  $\beta$ -catenin pathway. Elf3 binds to and transactivates the promoter of CTNNB1 ( $\beta$ -catenin), leading to  $\beta$ -catenin accumulation in cell nucleus. We acquired compelling data for the major regulatory role of Elf3 in  $\beta$ -catenin transactivation in CRC tissues. Finally, we explored the possibility of targeting Elf3 as a therapeutic measure to suppress CRC progression in xenograft mouse models. By these approaches we aim to elucidate the role of Elf3 in the regulation of  $\beta$ -catenin signaling and evaluate Elf3 as a potential biomarker for the prognosis CRC.

## Results

**Elf3 expression correlates with severity of CRCs.** We firstly investigated Elf3 expression level in normal colorectal

<sup>1</sup>State Key Laboratory of Oncogene and Related Genes, Key Laboratory of Gastroenterology & Hepatology, Ministry of Health, Department of Gastroenterology and Hepatology, Ren-Ji Hospital, School of Medicine, Shanghai Jiao-Tong University, Shanghai Cancer Institute, Shanghai Institute of Digestive Disease, 145 Middle Shandong Road, Shanghai, China and <sup>2</sup>Department of Surgery, University of Michigan, Ann Arbor, MI, USA

\*Corresponding author: J Xu or J-Y Fang, Department of Gastroenterology and Hepatology, Ren-Ji Hospital, School of Medicine, Shanghai Jiao-Tong University, Key Laboratory of Gastroenterology & Hepatology, Ministry of Health, Shanghai Institute of Digestive Disease, State Key Laboratory of Oncogene and Related Genes, Shanghai Cancer Institute, 145 Middle Shandong Road, Shanghai 200001, China. Tel: 0086-21-63200874; Fax: 0086-21-63266027; E-mail: xujieletter@gmail.com or jingyuanfang@yahoo.com

<sup>3</sup>These authors contributed equally to this work.

**Keywords:** Elf3;  $\beta$ -catenin; transactivation; colorectal cancer; prognosis

**Abbreviations:** Elf3, E74-like factor 3; Ets, E-twenty-six transcription factor; CRC, colorectal cancer

Received 22.1.14; revised 30.3.14; accepted 03.4.14; Edited by G Amarante-Mendes

tissues and CRC tissues by immunofluorescence and quantitative reverse transcription PCR (qRT-PCR) and found significant increase of Elf3 mRNA and protein levels in CRC tissues than in normal colorectal tissues ( $P < 0.001$ , two-sided student *t*-test, Figures 1a and b, Supplementary Figure S1a). By analyzing the CRC cohort in The Cancer Genome Atlas (TCGA), we found that the Elf3 gene (located in 1q32.1) is recurrently amplified in CRC (Figures 1c and d), and gained copy number variation significantly associates with increased mRNA expression level (Figure 1e). Of note, amplification of Elf3 gene has been previously found in breast cancers.<sup>17</sup> Moreover, the mRNA level of ELF3 increased progressively from normal colorectal mucosa to primary CRC and then to metastatic CRC (Figure 1f). These features suggest a scenario wherein Elf3 may have functional roles in the development of CRC.

To test whether Elf3 expression correlates with different clinicopathological features of CRC, 76 CRC patients were stratified by Elf3 expression as determined by immunofluorescence. Elf3 upregulation significantly associated with larger tumor size (diameter  $> 5$  cm,  $P = 0.03$ ) and lymph node invasion ( $P = 0.04$ , Supplementary Table 1). Interestingly, patients with high-Elf3 expression exhibited significantly shorter survival time ( $P = 0.03$ , 7-year follow-up, Kaplan–Meier test, Figure 1g). The prognostic significance of Elf3 was validated in an independent dataset, which consistently reported shorter survival for patients expressing higher level of Elf3 ( $P = 0.009$ , 10-year follow-up, Figure 1h). Taken together, these results demonstrate a tight association between Elf3 upregulation and poor CRC prognosis, and further support our notion that Elf3 may function as an oncogene in CRC development.

**CRC cells display addiction to Elf3 expression.** In light of the above findings, we questioned whether CRC cells require Elf3 expression to display strong malignant phenotypes. We found that CRC cells, HCT116 and SW1116 express higher levels of Elf3 (Supplementary Figure 1b), and thus have used specific small interfering RNAs (siRNAs) to knockdown Elf3 expression these cells. Efficient knockdown of Elf3 was detected in both mRNA and protein levels (Supplementary Figures 1c and d). Flow cytometry assay indicated that suppression of Elf3-induced cell cycle arrest of both HCT116 (Figures 2a and b) and SW1116 cells (Supplementary Figures S2a and b). In addition, knockdown of Elf3 also significantly increased the cells in sub-G1 phase (Figures 2b and Supplementary Figure S2b), and the increase in cell apoptosis was confirmed by PE-conjugated annexin V staining and FACS (Figures 2c and d and Supplementary Figure S2c). CCK-8 assay indicated that suppression of Elf3 significantly decreased the proliferation rate of HCT116 and SW1116 cell lines (Figures 2e and f). We further used Transwell assay to monitor the effect of manipulating Elf3 expression on cell invasiveness. Knockdown of Elf3 significantly decreased the number of HCT116 and SW1116 cells that penetrated the Transwell filter (Figures 2g and h), which suggested a substantial loss of cell invasion ability.

**Identification of  $\beta$ -catenin as a regulatory target of Elf3.** We next investigated the mechanism underlying the

pro-malignancy effects of Elf3. To assess the signaling fingerprint that specifically associates with the expression of Elf3 in CRC, we performed GSEA using expression profiling data of 390 CRC tissues (GEO accession GSE41258).<sup>18</sup> Interestingly, three gene sets related to Wnt/ $\beta$ -catenin were identified with the strongest association with Elf3 expression (Figure 3a).

Since Elf3 functions as a transcriptional factor, we explored the possibility if Elf3 may induce Wnt/ $\beta$ -catenin signaling by transactivating any key component in this pathway. In support of this, we found multiple putative Elf3-binding sites in the promoter region of  $\beta$ -catenin (Figure 3b). Moreover, both chromatin immunoprecipitation (ChIP) and electrophoretic mobility shift assay (EMSA) confirmed that Elf3 could indeed bind to the promoter of  $\beta$ -catenin (Figures 3c and d, Supplementary Figure S3a). When the  $\beta$ -catenin promoter sequence was cloned into a luciferase reporter, ectopic expression or knockdown of Elf3 increased and decreased, respectively the  $\beta$ -catenin promoter activity in both HCT116 and SW1116 cells ( $P < 0.001$ , Figure 3e and Supplementary Figure S3b). Nonetheless, the transactivity of Elf3 on  $\beta$ -catenin promoter was completely abolished after the putative Elf3-binding sites were mutated (Figure 3f and Supplementary Figure S3c), suggesting these sequence elements as true binders to Elf3. Consistently, qRT-PCR assay revealed that knockdown of Elf3 could significantly decrease the expression of  $\beta$ -catenin (Figure 3g and Supplementary Figure S3d), while ectopic expression of induced significant upregulation of  $\beta$ -catenin in both cell lines (Figure 3h and Supplementary Figure S3e). These data demonstrate  $\beta$ -catenin as a direct transcription target of Elf3, and explain the strong association of Elf3 with Wnt/ $\beta$ -catenin signaling.

**Elf3 potentiates Wnt/ $\beta$ -catenin signaling in CRC cells.** To test whether Elf3 could induce accumulation of Elf3 in CRC cells, we manipulated Elf3 expression and detected  $\beta$ -catenin protein level by Western Blot. As a result, ectopic expression or knockdown of Elf3 increased/decreased the level  $\beta$ -catenin protein in the whole cell, respectively (Figures 4a and b, Supplementary Figures S4a and b). As nuclear  $\beta$ -catenin is critical for the activation of wnt signaling pathway, we further analyzed  $\beta$ -catenin level in the nuclear protein fraction isolated from CRC cells. As expected, the nuclear  $\beta$ -catenin level was downregulated following siRNA-mediated Elf3 depletion and upregulated after Elf3 ectopic expression in both HCT116 and SW1116 cells (Figures 4c and d, Supplementary Figures S4c and d).

To test if Elf3-induced  $\beta$ -catenin expression may alter the functional status of the pathway, we analyzed  $\beta$ -catenin/TCF transcriptional activity using TOP Flash/FOP Flash and detected the levels of multiple downstream effectors in the Wnt/ $\beta$ -catenin pathway using qRT-PCR. The TOP/FOP assay suggested that  $\beta$ -catenin/TCF transcriptional activity was significantly decreased after knockdown of Elf3 and substantially increased upon Elf3 ectopic expression in both HCT116 (Figures 4e and f) and SW1116 cells (Supplementary Figures S4e and f). Moreover, the expression of selected Wnt pathway target genes (including c-Myc, VEGF, CCND1, MMP-7 and c-Jun) were significantly downregulated upon Elf3 depletion (Figure 4g, Supplementary Figure S4g), and were

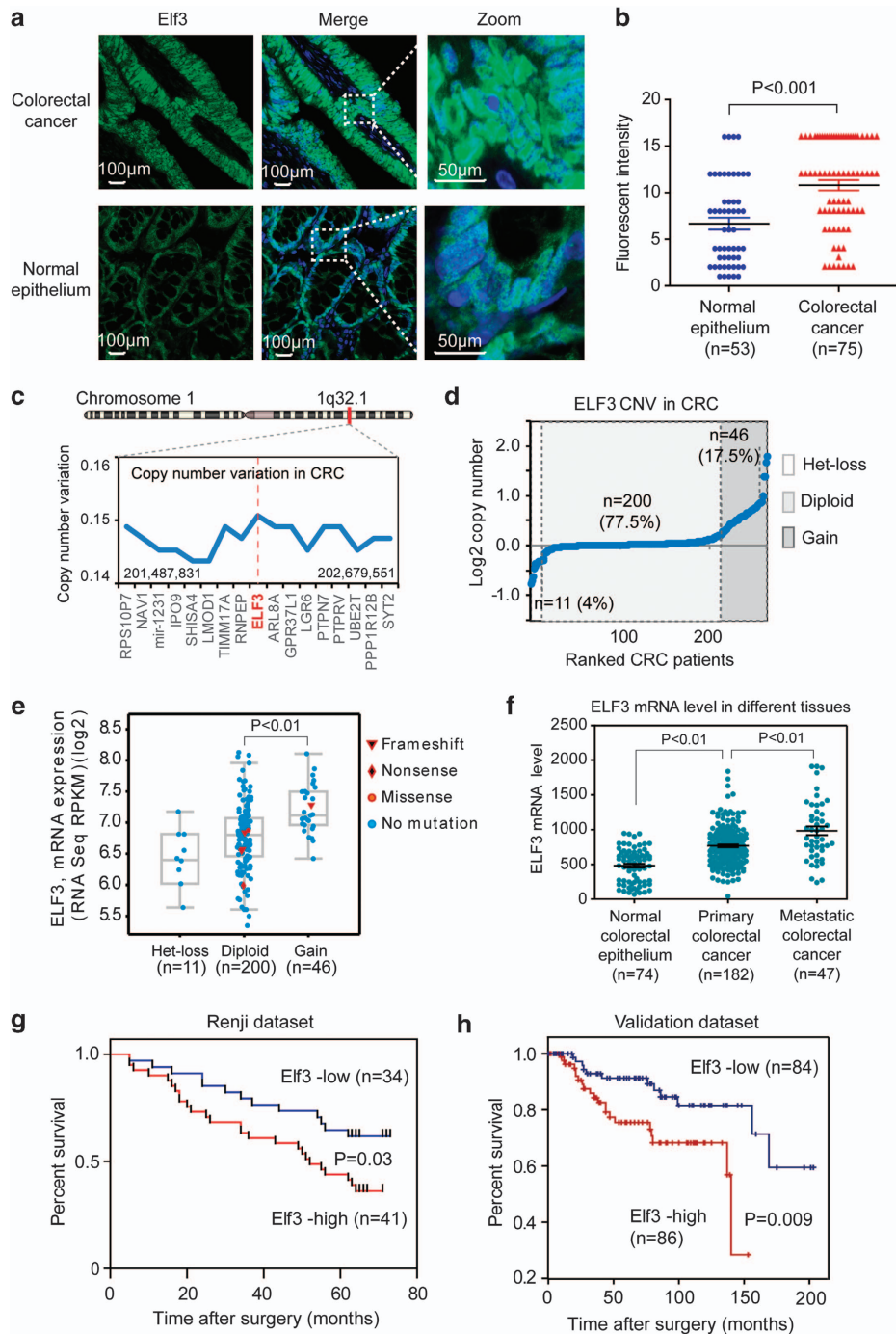


**Figure 1** Upregulation of Elf3 in CRC and its association with poor survival. (a) Immunofluorescence of Elf3 in normal and CRC tissues. Elf3 is labeled in green, and cell nucleus is stained by DAPI in blue. Scale bars indicate 100  $\mu$ m in normal panels (400  $\times$ ). (b) Statistics of Elf3 protein expression levels in normal and CRC tissues. The level of Elf3 protein was estimated according to immunofluorescence intensity and compared between normal and cancer tissues ( $P < 0.001$ , paired *t*-test). (c) Amplification of ELF3 gene in the genome of CRC tissues. The CNV data were obtained from CRC cohort of The Cancer Genome Atlas (TCGA) database, and the plot shows mean CNV of each gene in the indicated genomic region (1q32.1). Elf3 sits in a peak for gained CNV in the region. (d) The copy number variations of ELF3 gene in all patients from the TCGA CRC cohort are shown in the plot (log<sub>2</sub> ratios, cancer versus normal). Patients are ranked according to CNV of ELF3 gene, and putative copy numbers are indicated on the right (het-loss, diploid or gain). (e) Gained CNV of ELF3 gene associates with upregulated mRNA expression. The plot shows ELF3 mRNA levels (obtained from microarray data) in patients bearing different copy numbers of ELF3 gene (het-loss, diploid or gain). Significantly higher ELF3 mRNA levels are found in patients carrying gained ELF3 copy numbers ( $P < 0.01$ , Mann–Whitney test). (f) The ELF3 mRNA level is progressively upregulated in primary and metastatic colorectal cancer tissues. The expression of ELF3 mRNA was obtained from the Isreali cohort (GSE41258), and compared between different groups including normal colorectal epithelium, primary CRC, and metastatic CRC ( $P < 0.01$ , Mann–Whitney test). (g) Kaplan–Meier survival plot of patients stratified by Elf3 protein expression level. In this 7-year follow-up study, patients expressing higher level of ArhGAP30 displayed shorter overall survival than the other patients ( $P = 0.03$ , Kaplan–Meier survival test). (h) Association between Elf3 expression and survival of CRC patients in an independent validation dataset (Israeli cohort, 10-year follow-up). The CRC patients were stratified according to mRNA Elf3 expression level (median split) into Elf3-high and Elf3-low groups. Patients expressing high-Elf3 level displayed significantly shorter survival ( $P = 0.009$ , Kaplan–Meier survival test).

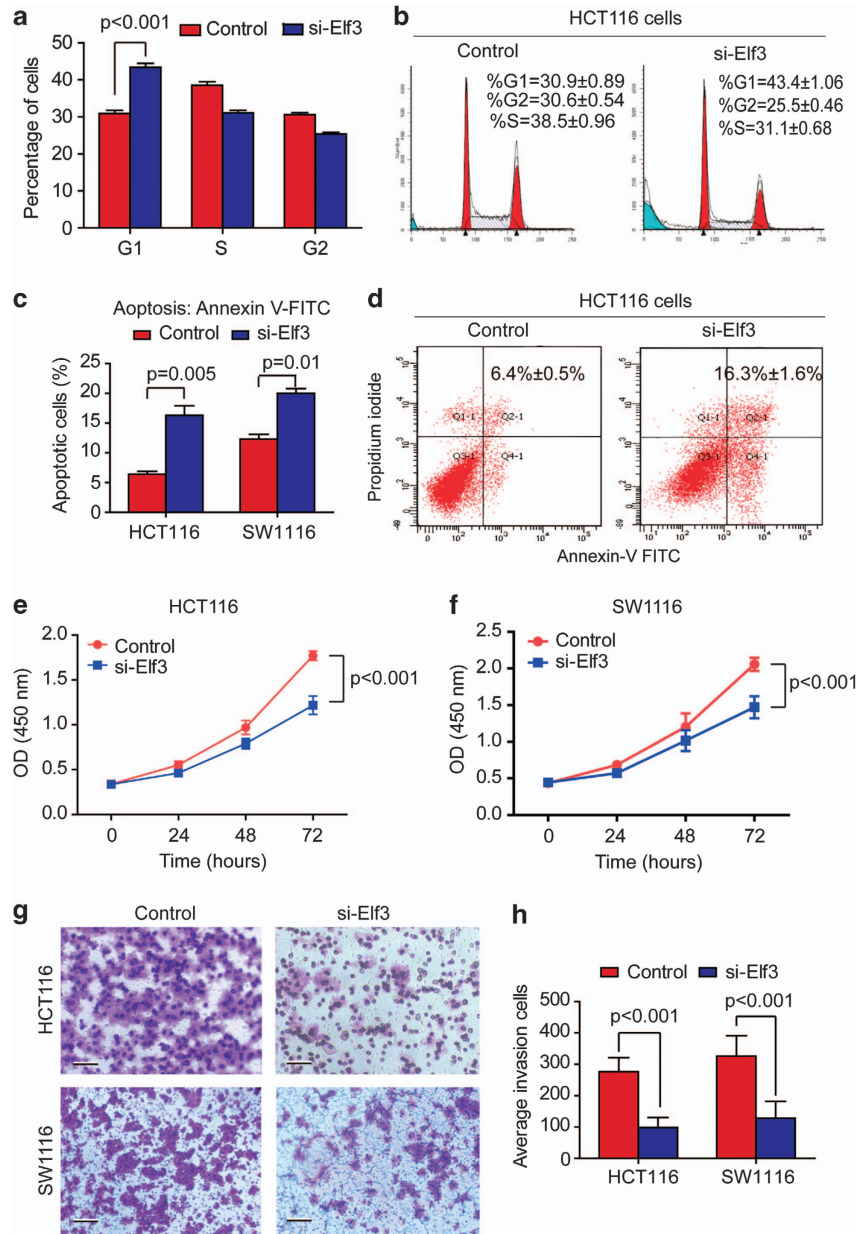


**Figure 2** Knockdown of Elf3 suppresses invasion and proliferation and induces apoptosis and cell cycle arrest of colorectal cancer cells. The HCT116 and SW1116 cells were transiently transfected with Elf3 siRNA or control siRNA for subsequent analyses. Data in all statistical plots represent means  $\pm$  S.D. (**a**, **b**) Flow cytometry assay of HCT116 cells treated by Elf3 siRNA. The knockdown of Elf3 induced significant increase of cells in sub-G1 and G1 phases as compared with control siRNA. The statistics of cell cycle distribution are shown in (**a**) and representative FACS images are shown in (**b**). (**c**, **d**) Apoptosis of HCT116 and SW1116 cells induced by Elf3 knockdown. Flow cytometric assay based on phycoerythrin (PE)-conjugated annexin V staining showed increased apoptosis of HCT116 and SW1116 cells treated by Elf3 siRNA. Statistics based on 3 independent experiments is shown in (**c**), and representative FACS images are shown in (**d**). (**e**, **f**) Proliferation curves of HCT116 (**e**) and SW1116 cells (**f**) as determined by CCK-8 assay. Significant difference in cell viability was found 72 h after cell plating ( $P < 0.001$ , two-sided *t*-test). (**g**, **h**) Knockdown of Elf3 suppressed migration of CRC cells. The HCT116 and SW1116 cells were transfected by Elf3 siRNAs, and transwell assay was applied to quantify cell migration ability. Statistical result based on three independent experiments is indicated in (**g**), and representative transwell cell staining images are shown in (**h**)

upregulated in response to Elf3 overexpression (Figure 4h, Supplementary Figure S4h). These effector genes have well-established roles in malignant transformation and cancer progression,<sup>19–22</sup> thus could provide mechanistic explanation for the pro-malignant effects of Elf3.

**Elf3 confers  $\beta$ -catenin-dependent effects on CRC cell aggressiveness.** Interestingly, knockdown of Elf3 in both

HCT116 and SW1116 cells increased cell apoptosis, while ectopic expression of  $\beta$ -catenin blocked this effect (Figures 5a–c). Moreover, Elf3 knockdown decreased cell invasion and proliferation, while upregulation of  $\beta$ -catenin restored cell invasion (Figures 5d and e) and proliferation (Figures 5f and g). These findings suggest that Elf3 increases CRC aggressiveness in a  $\beta$ -catenin-dependent manner.



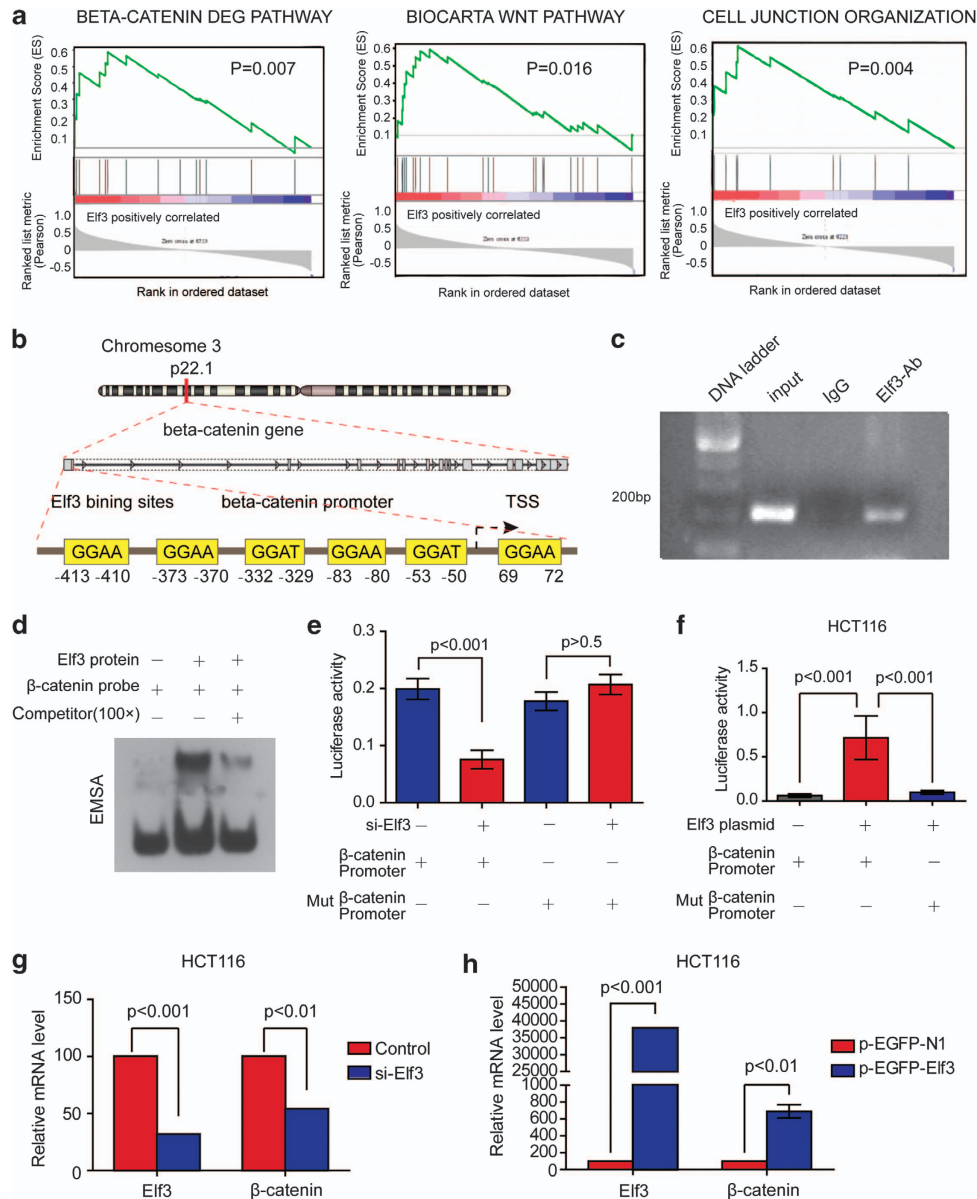


**Figure 3** Identification of  $\beta$ -catenin as regulatory target of Elf3. (a) GSEA showing the association between Elf3 expression and activity of the Wnt/ $\beta$ -catenin signaling pathway. Gene expression profiling data from the Israeli cohort was analyzed by GSEA using ELF3 expression as phenotypic label for identification of enrichment pathways among different curated gene sets. The signatures ' $\beta$ -catenin deregulation', 'Wnt pathway' and 'cell junction organization (actually also linked to Wnt/ $\beta$ -catenin signaling)' were found significantly associated with Elf3 expression. (b) Location of the Elf3-binding sites of the  $\beta$ -catenin promoter. The  $\beta$ -catenin gene promoter contains multiple binding sites for Elf3 (highlighted in yellow) in the region between  $-413$  and  $+72$  bp in relation to the transcription starting site. This DNA sequence was inserted into the PGL3 luciferase reporter to test the transactivity of Elf3 to  $\beta$ -catenin. (c) ChIP assay showing the binding of Elf3 to  $\beta$ -catenin promoter *in vivo*. The Elf3 protein was pulled down in HCT116 cells, and specific primers were used to amplify the  $\beta$ -catenin promoter in the recovered DNA from the IP complex. The input DNA and ChIP yield using nonspecific IgG are included as controls. (d) EMSA assay showing the binding of Elf3 to  $\beta$ -catenin promoter *in vitro*. (e, f) The luciferase reporter assay suggested that Elf3 can transactivate the  $\beta$ -catenin promoter ( $-413$  to  $+72$  bp) but not the mutant sequence devoid of the putative binding sites. The HCT116 cells were transfected with Elf3 siRNA (e) or Elf3 plasmid (f), and luciferase activity is calculated by the ratio of firefly (reporter)/renilla (normalization) signals. (g, h) qRT-PCR assay showing Elf3 could transactivate  $\beta$ -catenin in colorectal cancer cells. The HCT116 cells were transfected with Elf3 siRNA (g) or Elf3 plasmid (h), and detected for the level of  $\beta$ -catenin by qRT-PCR. Data represent means  $\pm$  S.D. ( $P < 0.01$ , two-sided *t*-test)

**Elf3 strongly associates with  $\beta$ -catenin expression in CRC tissues.** To test the physiological occurrence of Elf3-induced  $\beta$ -catenin in CRC, we detected and analyzed the correlation between Elf3 and  $\beta$ -catenin expression in CRC tissue samples. Firstly, qRT-PCR revealed that both Elf3 and  $\beta$ -catenin are substantially upregulated in

CRC tissues when compared with normal tissues ( $P < 0.001$ , Figure 6a), and significant positive correlation was found between Elf3 and  $\beta$ -catenin mRNA levels in CRC ( $R = 0.6107$ ,  $P < 0.001$ ; Figure 6b). By immunofluorescent co-staining of Elf3 and  $\beta$ -catenin, we found that CRC tissues expressing higher levels of Elf3 expression also

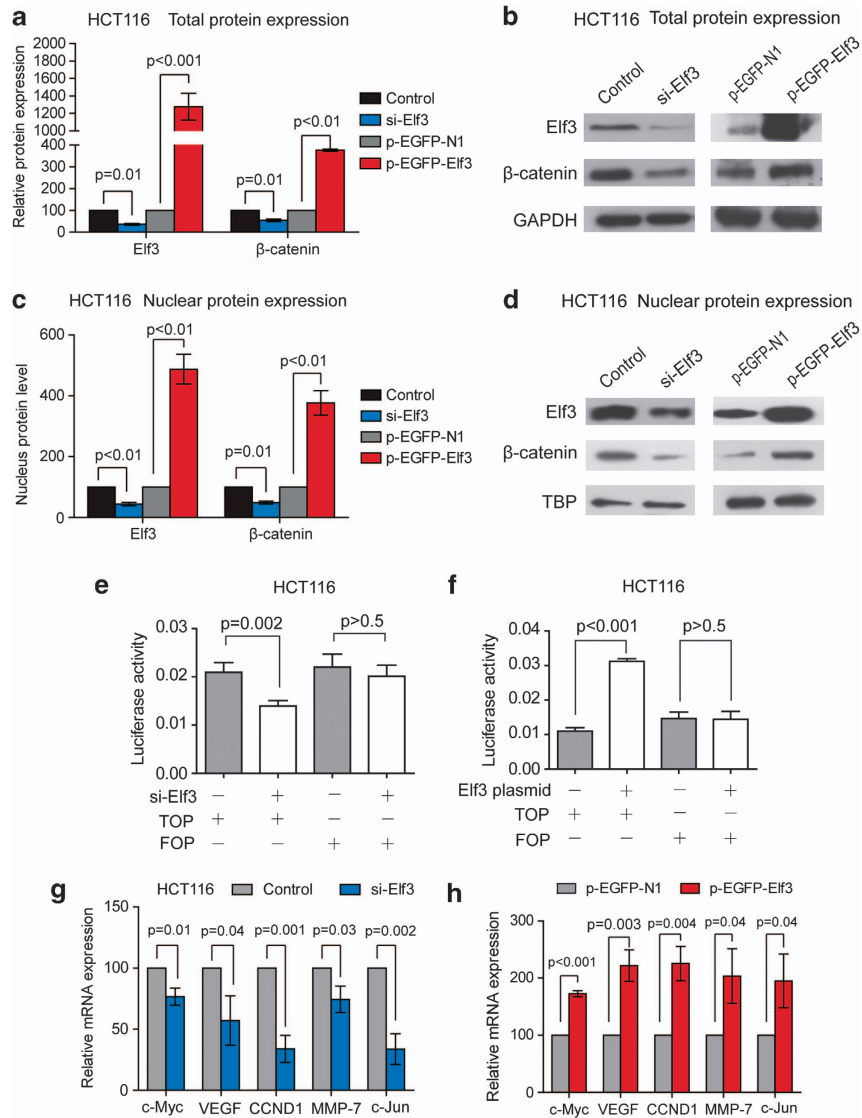


**Figure 4** Elf3 enhances the Wnt/ $\beta$ -catenin signaling pathway in CRC cells. (**a**, **b**) Representative Western blot and summarized data show that Elf3 siRNA transfection significantly decreases total  $\beta$ -catenin expression, while Elf3 overexpression significantly increased total  $\beta$ -catenin levels in HCT116 cells. Statistical result based on three independent experiments is indicated in (**a**), and representative western blot images are shown in (**b**). (**c**, **d**) Representative Western blot and summarized data show that Elf3 siRNA transfection significantly decreases nuclear  $\beta$ -catenin expression, while Elf3 overexpression significantly increased nuclear  $\beta$ -catenin levels in HCT116 cells. Statistical result based on three independent experiments is indicated in (**c**), and representative western blot images are shown in (**d**). (**e**, **f**) TOP/FOP flash assays indicate that Elf3 knockdown significantly reduces the  $\beta$ -catenin/TCF transcriptional activity (**e**), while Elf3 overexpression significantly increases the  $\beta$ -catenin/TCF transcriptional activity in HCT116 cells (**f**). (**g**, **h**) qRT-PCR assay showing Elf3 could transactivate the Wnt/ $\beta$ -catenin downstream genes in CRC cells. Knockdown of Elf3 could suppress the expression of Wnt/ $\beta$ -catenin target (c-Myc, VEGF, CCND1, MMP-7 and c-Jun) downstream (**g**), while ectopic expression of Elf3 transactivated these downstream genes (**h**)

display stronger positivity for  $\beta$ -catenin ( $P = 0.0002$ , Figures 6c–e). These data collectively demonstrate a key role of Elf3 in  $\beta$ -catenin regulation in CRC.

**Targeting Elf3 efficiently suppresses xenograft growth in mice.** We found that knockdown of Elf3 suppressed the growth of both HCT116 and SW1116 cells in soft agar colony formation assays (Figures 6f and g). To further confirm the impact of Elf3 on  $\beta$ -catenin expression and tumor growth *in vivo*, we established a HCT116 xenograft tumor model in BALB/C nude mice. The human CRC HCT116 cells were

implanted subcutaneously into athymic nude mice to allow tumor formation, and specific siRNAs for Elf3 (or control siRNAs) were periodically delivered into tumor cells via an *in vivo* transfection vehicle. As a result, the xenograft tumor volume was significantly smaller in si-Elf3 group than in the control group ( $P < 0.001$ , Figures 7a–c), indicating that Elf3 knockdown significantly suppresses CRC tumor growth *in vivo*. Knockdown of Elf3 also substantially decreased the level of  $\beta$ -catenin in xenograft tumors, which supported our notion that Elf3 is required for the accumulation of  $\beta$ -catenin in CRC (Figures 7d–f). These data, together

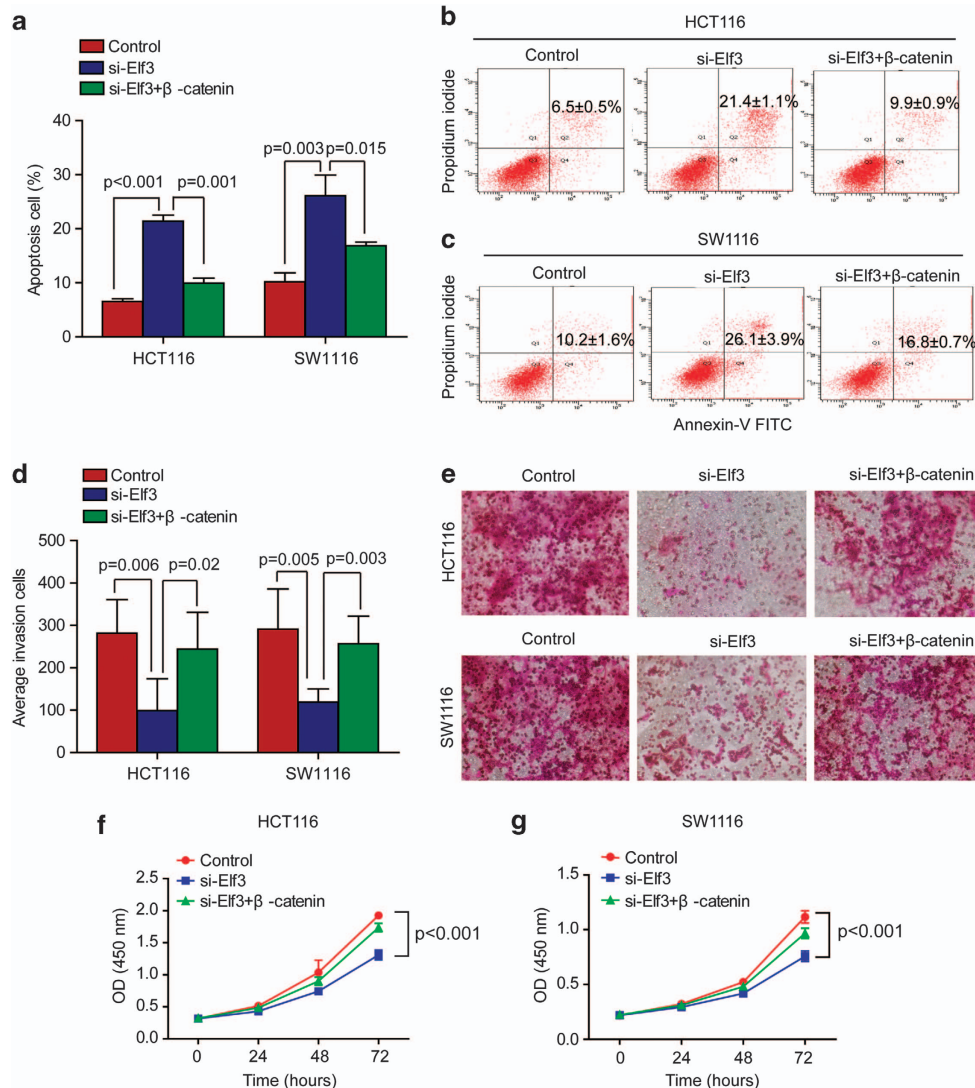


**Figure 5** Expression of  $\beta$ -catenin rescues CRC cell malignant phenotypes that were suppressed by knockdown of Elf3. **(a)** The statistical analysis of CRC cell apoptosis in different experimental groups. The HCT116 and SW1116 cells were treated by specific siRNAs for Elf3 expression in the absence or presence of  $\beta$ -catenin expression vector. Statistical result based on three independent experiments (*P*-values indicated, *t*-test). **(b, c)** Representative flow cytometry images in experiments described above. **(d, e)** Statistical result and representative images of Transwell assay of HCT116 and SW116 cells treated by specific siRNAs for Elf3 expression in the absence or presence of  $\beta$ -catenin expression vector. **(f, g)** Proliferation of HCT116 and SW1116 cells treated by specific siRNAs for Elf3 expression in the absence or presence of  $\beta$ -catenin expression vector (*P*-values indicated, *t*-test)

with the recurrent amplification and upregulation of Elf3 in CRC, suggest that targeting Elf3 may have therapeutic potential in CRC.

## Discussion

As a major effector in the Wnt oncogenic pathway,  $\beta$ -catenin is thought to be regulated mainly at the protein level, and mechanisms for transcriptional regulation of  $\beta$ -catenin have received little attention to date. By investigating the roles of Elf3 in CRC, our results identify an alternative mechanism for  $\beta$ -catenin accumulation that involves direct transactivation by Elf3. In addition, our study also brings the prognostic significance of Elf3 into attention.

We found that Elf3 functions as an Ets transcription factor that confers transcriptional regulation of wnt/ $\beta$ -catenin

signaling in CRC. Aberrant regulation of the Wnt/ $\beta$ -catenin pathway has an important role during the onset and progression of CRC, with over 90% of cases of sporadic colon cancer featuring APC mutations and  $\beta$ -catenin accumulation, and accessed  $\beta$ -catenin translocates to the nucleus driving LEF/TCF-mediated gene transcription.<sup>23</sup> While the ubiquitin-mediated degradation is widely accepted as a major regulatory mechanism at the protein level, little is known about the regulation of  $\beta$ -catenin at transcriptional level. In fact, only a few previous studies have provided evidence for a transcriptional mechanism of  $\beta$ -catenin regulation.<sup>24,25</sup> Here our study provides solid evidence for a transcriptional mechanism of  $\beta$ -catenin regulation in CRC carcinogenesis. The ChIP, EMSA and luciferase assays revealed that Elf3 could bind to the promoter of  $\beta$ -catenin and transactivate its transcription. Consistently, manipulating Elf3 also influences

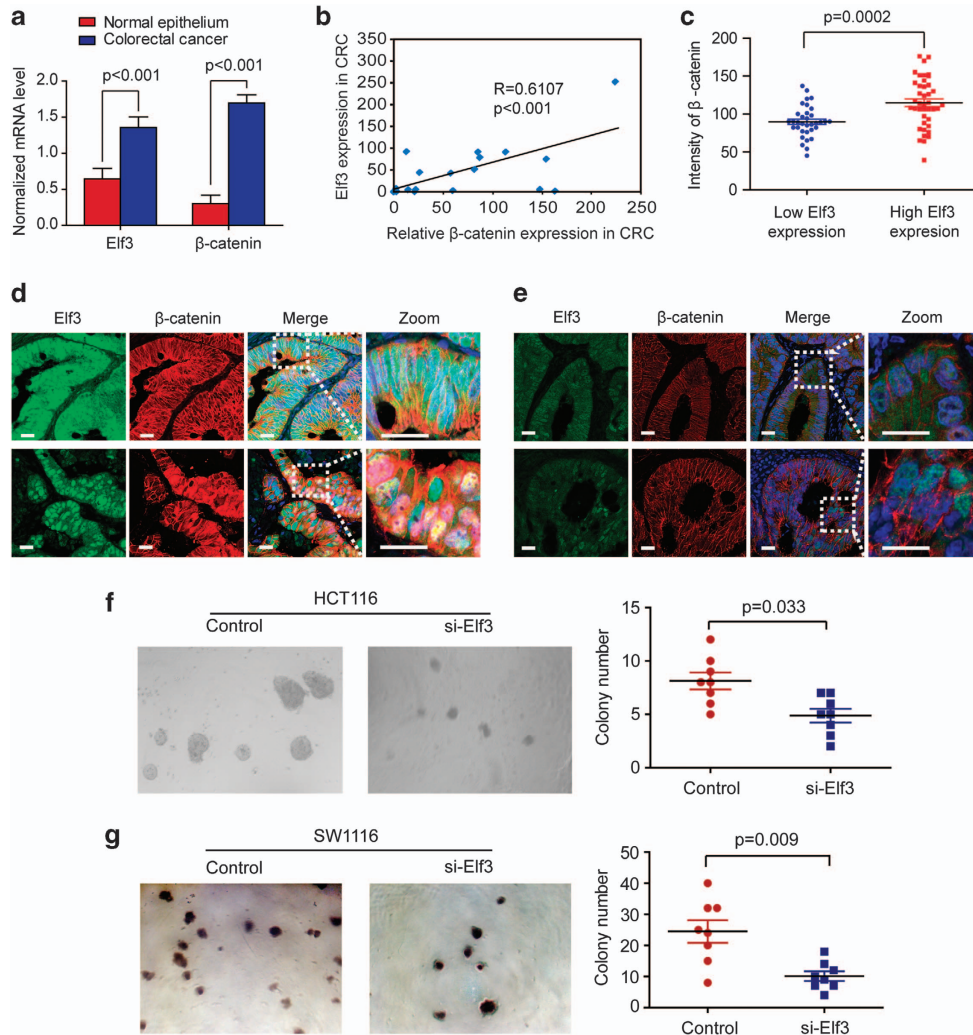


**Figure 6** Elf3 associates with  $\beta$ -catenin accumulation in CRC tissues. (a) qRT-PCR assay showing that both Elf3 and  $\beta$ -catenin mRNA are significantly elevated in CRC tissues when compared with matched normal tissues. (b) Regression analysis reveals a positive correlation between Elf3 and  $\beta$ -catenin mRNA expression in CRC tissues ( $R = 0.6107$ ,  $P < 0.001$ ). (c) Statistical summary for the tissue staining of Elf3 and  $\beta$ -catenin in CRC tissues. The expression of  $\beta$ -catenin was generally higher in CRC tissues with stronger Elf3 staining than that in weaker Elf3 staining ( $P = 0.0002$ , Mann-Whitney test). (d, e) Representative immunofluorescent images of Elf3 and  $\beta$ -catenin in human CRC tissues. Specific antibodies were used to label Elf3 protein in green and  $\beta$ -catenin in red, respectively. The zoomed sections are shown on the right. Representative staining images for Elf3-high expression tissues are shown in (d), and images for Elf3-low tissues are shown in (e). (f, g) Soft agar colony formation assay showing the effect of Elf3 knockdown on the proliferation of HCT116 and SW1116 cells. The representative images have been shown on the left panels, while statistical results are shown on the right

the translocation of  $\beta$ -catenin and  $\beta$ -catenin/TCF transcriptional activity (mechanistic model shown in Figure 7g). Moreover, the strong effect of Elf3 on  $\beta$ -catenin transcription was systemically validated *in vivo*. Targeting Elf3 in xenograft mouse models substantially decreased the  $\beta$ -catenin level, and the expression level of Elf3 strongly correlated with  $\beta$ -catenin level in human CRC tissues. These compelling data stress the importance of Elf3 in the regulation of  $\beta$ -catenin expression and activity of this oncogenic signaling pathway in CRC.

First, our data reveals Elf3 as a promising biomarker for the prognosis of CRC. We found that Elf3 is progressively upregulated in primary and metastatic CRC tissues, and Elf3 overexpression associates with poor CRC patient survival in both our results and an independent validation dataset. Of note, recent studies have pointed to a link between Elf3 expression

and inflammation,<sup>26,27</sup> thus the upregulation of Elf3 in CRC might also be relevant to inflammatory signaling in the colorectal epithelium. Moreover, the expression of Elf3 protein can be conveniently detected by immunohistochemistry of endoscopic biopsy specimens. Thus, it is worthy to study the prognostic effect of Elf3 in CRC in future prospective studies.

Moreover, the recurrent amplification of Elf3 gene in CRC, together with the requirement Elf3 for maintaining the aggressive phenotypes of CRC cells, strongly suggest the oncogenic roles of Elf3 in CRC. Thus, targeting Elf3 might provide alternative opportunity to inhibit the progression of CRC. The CRC xenograft models in this study revealed that suppressing Elf3 could significantly delay tumor growth *in vivo*, thus adding further support to the potential of Elf3 as a therapeutic target in CRC.



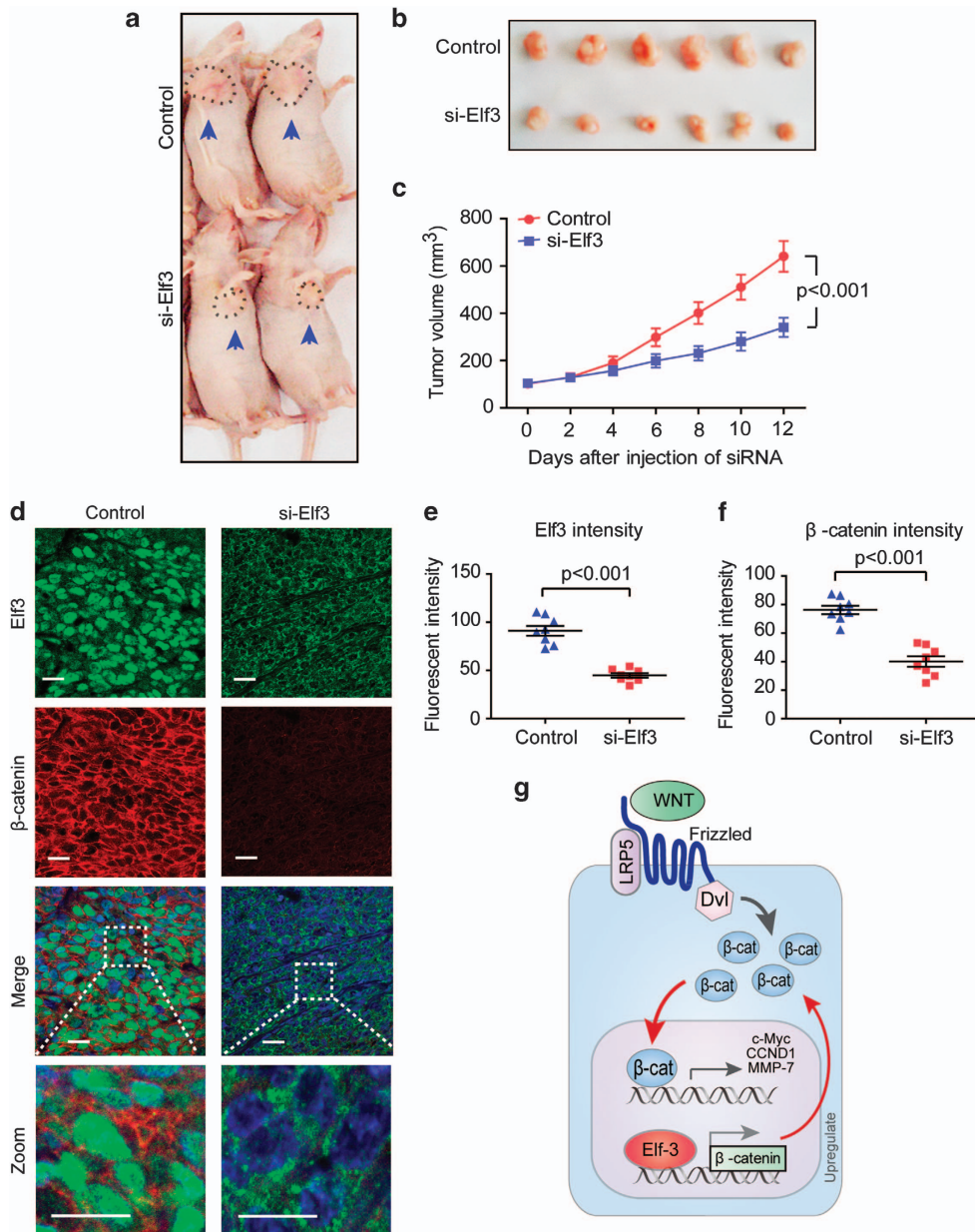


**Figure 7** Elf3 could serve as a potential therapeutic target in CRC. **(a,b)** Knockdown of Elf3 inhibited growth of xenograft in nude mice. Human CRC HCT116 cells were injected subcutaneously into the right armpit to establish a xenograft model, and specific siRNA for Elf3 or control siRNA was introduced to tumors cells by *in vivo*-jetPEI nanoparticles. The sizes of *in situ* and resected tumors treated with/without Elf3 siRNAs in the last time point (12 days after first injection) are shown in panels **(a)** and **(b)**, respectively. **(c)** Tumor growth curves in the Elf3 siRNA group and the control group ( $P < 0.001$ , *t*-test for tumor sizes at the last time point). Knockdown of Elf3 significantly suppressed xenograft tumor progression. **(d-f)** Immunofluorescence showing knockdown of Elf3 dramatically decreased the level of  $\beta$ -catenin in xenograft CRC tumors. Representative immunofluorescence images are shown in **(d)**, Statistical results are indicated in **(e)** and **(f)**. **(g)** Proposed model for Elf3-mediated  $\beta$ -catenin signaling. The amplification of ELF3 gene in colorectal epithelial cells leads to upregulation of Elf3 mRNA, causing transactivation of  $\beta$ -catenin. In synergy with the well-established Wnt-dependent regulation at protein level, Elf3 induces substantial accumulation of  $\beta$ -catenin in CRC cells, leading to upregulation of pro-oncogenic effector genes (c-myc, CCND1, MMP-7, etc) and increased malignant phenotypes

In conclusion, our data shed light on the oncogenic roles of Elf3 in CRC, and add another important piece of information to the molecular underpinning of  $\beta$ -catenin activation during colorectal carcinogenesis. Our results also highlight Elf3 as a promising biomarker and therapeutic target for CRC.

#### Materials and Methods

**Patients and CRC biopsy specimens.** A total of 20 pathologically confirmed CRC patients were enrolled and underwent surgery at Ren-ji Hospital,

affiliated to the Shanghai Jiao-tong University School of Medicine, between December 2009 and April 2010. The study was approved by the ethics committee of Shanghai Jiao-tong University School of Medicine, and written informed consent was obtained from all patients at study entry. One tissue microarrays including 90 pairs of CRC and corresponding non-tumor tissues are purchased from BioChip (Shanghai, China).

**Immunofluorescence analysis of Elf3 and  $\beta$ -catenin.** Methods for tissue immunofluorescence have been described previously.<sup>28,29</sup> Briefly the tissue sections were deparaffinized in xylene and rehydrated

using a graded series of ethanol. All slides were treated with NaBH<sub>4</sub> to suppress autofluorescence of tissues. The expression levels of Elf3 and  $\beta$ -catenin were probed with the primary antibodies [Elf3 (Sigma, St. Louis, MO, USA), dilution 1:50;  $\beta$ -catenin (CST, Beverly, MA, USA) dilution 1:400] according to the manufacturer's instructions. Secondary antibodies (Alexa488-anti-rabbit and Alexa546-anti-mouse) were used to label Elf3 and  $\beta$ -catenin, respectively. After staining with DAPI (1:2000), the coverslips were added with antifade reagent (ProLong Gold, Invitrogen, Carlsbad, CA, USA) and kept in the dark for 24 h. Images were acquired with a confocal fluorescence microscope (Carl Zeiss, Jena, Germany). Protein expression was quantified based on staining intensity, and divided into four grades: 1, negative; 2, weakly staining; 3, moderately positive; 4, strong positive.

**Cell lines and culture conditions.** The human CRC cell lines, HCT116 and SW1116 (ATCC, Manassas, VA, USA) were maintained in McCoy5A, RPMI 1640 medium (Gibco, Gaithersburg, MD, USA) supplemented with 10% fetal bovine serum (Invitrogen) and cultured in a humidified incubator at 37 °C under 5% CO<sub>2</sub>.

**RNA interference.** Commercial siRNAs specifically targeting Elf3 (GenBank Accession Number: NM\_004433) were synthesized by GenePharma (Shanghai, China) using the following sequence: siRNA-1: 5'-GCUACCAAGUGGAGAAGA ATT-3'; siRNA-2: 5'-GCCAUGAGGUACUACUACATT-3'; siRNA-3: 5'-UCAUUGA GCUGCUGG AGAATT-3'. These siRNAs were used as a pool for siRNA transfection. For siRNA transfection, HCT116 and SW1116 cells were seeded into normal growth medium at 30% confluence in six-well tissue plates 24 h before transfection, and then transfected with 5 nM siRNA (si-Elf3) using Lipofectamine 2000 Reagent (Invitrogen) in accordance with the manufacturer's instructions. Nonspecific siRNA (si-negative; GenePharma) was used as negative control. After 48 h, cells were harvested for analysis.

**Plasmids construction and transfection.** The pEGFP-Elf3 plasmid containing the Elf3 coding sequence was purchased from Shanghai GeneChem (Shanghai, China) and verified by DNA sequencing. For plasmid transfection, HCT116 and SW1116 cells were seeded into six-well plates 24 h before transfection, and then transfected with plasmids (4  $\mu$ g per well) using Lipofectamine 2000 Reagent (Invitrogen), according to the manufacturer's instructions. The pEGFP-N1 was used as an empty vector control. After 48 h, cells were harvested for analysis.

**qRT-PCR analysis.** Total RNA was extracted from 20 pairs of matched human CRC specimens (including cancer and adjacent nontumorous tissues) using TRIzol reagent (Invitrogen). All tissue samples were examined histologically, and all matched non-tumor tissues (taken at least 5 cm from the tumor) were confirmed to be normal. Reverse transcription was done using the First Strand cDNA Synthesis Kit (Takara, Shiga, Japan), according to the manufacturer's protocol. qPCR was performed using an ABI Prism 7900HT Sequence Detection System (Applied Biosystems, Grand Island, NY, USA) with SYBR Premix Ex Taq II (Takara). Quantification was calculated using the 2<sup>- $\Delta$ ACT</sup> method and is presented as fold change. The expression of each target gene was normalized to that of 18S RNA. Primer sequences were: Elf3 (forward, 5'-CACTGATGGC AAGCTCTTC-3'; reverse, 5'-GGAGCGCAGGA ACTTGAAG-3');  $\beta$ -catenin (forward, 5'-AGGTCTGAGGAGCAGCTTCA-3'; reverse, 5'-ATTGTCCACGCTGG ATTTTC-3'); 18S (forward, 5'-CGGACAGGAT T GACAGATTGATAGC-3'; reverse, 5'-TGCCAGAGTCTCGTTCTGTTATCG-3'); c-Myc (forward, 5'-GGCTCCTGGCA AAAGGTCA-3'; reverse, 5'-CT G GTA GTT GTGCTGATGT-3'); VEGF (forward, 5'-CGCAAAGTGTGTAACGGAATAG-3'; reverse, 5'-TCCAGAGGAGGAGTATGT GTGA-3'); c-Jun (forward, 5'-AAACGACCTTCTATGACGATGC-3', reverse, 5'-CCGTTGCTGGACTGGATT AT-3'); CCND1 (forward, 5'-GCTGCGAAGTG GAAACCATC-3', reverse, 5'-CCTCCTTCTGCACACATTTGAA-3'); MMP-7 (forward, 5'-GAGGCATGAGTG AGTACAGTG-3', reverse, 5'-ACATCTGGGCTTCTGCA TTATT-3').

**Western blot assay.** Whole cell lysates were prepared from the cancer cell lines and standard Western blotting analysis was performed using anti-Elf3 (R&D systems, Minneapolis, MN, USA), anti- $\beta$ -catenin (CST), and anti-GAPDH (Kangchen Biotechnology, Shanghai, China) antibodies. All primary antibodies were used at a 1:1000 dilution. Peroxidase-conjugated anti-goat or anti-rabbit IgG secondary antibodies were obtained from Kangchen Biotechnology and

used at a 1:5000 dilution. Three independent experiments were done for each analysis.

**Flow cytometry.** For cell cycle analysis,  $\sim 1 \times 10^6$  cells were fixed in cold ethanol at -20 °C overnight, and then incubated with propidium iodide for 30 min before analysis. For measuring the rate of apoptosis,  $\sim 5 \times 10^5$  cells were analyzed using an ApoAlert Annexin V-FITC Apoptosis kit (BD Clontech, Palo Alto, CA, USA) according to the manufacturer's instructions.

**Cell proliferation assay.** HCT116 or SW1116 cells ( $5 \times 10^3$  cells per well) were plated into triplicate wells of 96-well plates before si-Elf3, si-negative transfection or pEGFP-Elf3 and pEGFP-N1. Cell proliferation was assessed after 24, 48, 72 and 96 h using cell Counting Kit-8 (Dojindo, Tokyo, Japan) according to the manufacturer's instructions.

**Transwell assay.** Cell invasion assays were performed using Boyden chambers with filter inserts (pore size, 8  $\mu$ m) coated with 40  $\mu$ g matrigel in 24-well plate dishes. Briefly,  $2 \times 10^5$  HCT116 or SW1116 cells transfected with si-Elf3 or control siRNA were seeded in the upper chamber, while the medium with 20% fetal bovine serum was placed in the lower chamber. The plates were incubated for 24 h. Then the cells were fixed in 4% formaldehyde and stained with 0.1% crystal violet in PBS for 30 min at room temperature. Cells on the upper side of the filters were removed by cotton-tipped swabs, and the filters were washed with PBS. The cells on the lower side of the filters were defined as invasive cells and counted at  $\times 200$  magnification in 10 different fields of each filter.

**Soft agar colony formation assay.** The HCT116 and SW1116 cells ( $2 \times 10^3$ ) treated with si-Elf3 or control siRNA were plated into 24-well plates with 1% base agar and 0.5% top agar, and incubated for 2 (SW1116) or 3 weeks (HCT116). The colonies were counted in eight randomly microscope fields.

**Luciferase assays.** The  $\beta$ -catenin promoter was amplified by PCR and ligated into the pGL3-basic vector. The pRL-CMV encoding the Renilla luciferase for normalization is commercially available from Promega (Madison, WI, USA). HCT116 and SW1116 cells were seeded into 12-well-tissue plates 24 h before transfection, and then transfected with 5 ng siRNA or 1  $\mu$ g plasmid using the Lipofectamine 2000 Reagent (Invitrogen), according to the manufacturer's instructions. Plasmids transfection was done using Lipofectamine 2000 Reagent 1 day later. After another 48 h, cells were assayed using the Dual-Luciferase reporter assay system kit (Promega), as described previously.<sup>30</sup> All experiments were performed in triplicate and data were pooled from three independent experiments.

**TOP Flash/FOP Flash assay.** To evaluate the TCF/LEF transcriptional activity, we used a pair of luciferase reporter constructs, TOP Flash and FOP Flash (Millipore, Billerica, MA, USA). The TOP Flash contains three copies of TCF/LEF binding site, and FOP Flash contains a mutated TCF/LEF binding site. HCT116 and SW1116 cells were seeded into 12-well-tissue plates 24 h before transfection, and then co-transfected with 5 ng siRNA (control siRNA or si-Elf3) or Elf3 plasmid and 1  $\mu$ g plasmid (TOP Flash or FOP Flash) using the Lipofectamine 2000 Reagent (Invitrogen), according to the manufacturer's instructions. After 48 h, cells were assayed using the Dual-Luciferase reporter assay system kit (Promega), according to the manufacturer's instructions. The results are normalized to Renilla luciferase activity.

**Chromatin immunoprecipitation assay.** ChIP assays have been described previously.<sup>31</sup> Briefly, immunoprecipitation were performed using a ChIP kit (Millipore), according to the manufacturer's instructions. Briefly,  $1 \times 10^6$  cells and 5  $\mu$ g anti-Elf3 antibody were used for each ChIP experiment. Goat serum was used as a negative control. The DNA sequence surrounding the Ets-binding site in the human  $\beta$ -catenin promoter was amplified from immunoprecipitated protein-DNA complexes using the following primer pair: (forward, 5'-ACCTCCATACA TACC-3'; reverse, 5'-CAGGTGCTTCTGCTGT-3').

**Electrophoretic mobility shift assay (EMSA).** The biotin labeled oligonucleotides of  $\beta$ -catenin probe and unlabeled probe were synthesized from Sangon Biotech (Shanghai, China). The Elf3 recombinant protein was purchased

from Abnova (Taipei City, Chinese Taipei). The chemiluminescent EMSA kit was purchased from Beyotime Institute of Biotechnology (Shanghai, China). This experiment was performed according to the manufacturer's instructions. The sequence (5'-3') of the probe used in the EMSA was: GCATGGATTGGTGAGGGGCAGGGGAAAG.

**In vivo experiments.** Briefly, male BALB/c athymic nude mice (4–6 weeks old) were obtained from the Experimental Animal Center of SIBS. All mice were injected subcutaneously into the right armpit with  $1.0 \times 10^7$  HCT116 cells to establish a CRC xenograft model. Six days after subcutaneous inoculation, mice were randomly divided into two groups (six mice per group) and subjected to multi-point intratumoral injections ( $10 \mu\text{l}$  at three points) of siRNA or control siRNA complexed with the *in vivo*-jetPEI (Polyplus-transfection Inc., New York, NY, USA) transfection reagent. siRNA injections were administered every 2 days. After six sets of injections, all mice were sacrificed and subcutaneous tumors were collected for analysis. Detailed methods were published previously.<sup>20</sup> Our study was approved by the Animal Care and Use Committee of the Shanghai Jiao-Tong University School of Medicine Ren-Ji Hospital, Shanghai, China. All animal procedures were performed according to the guidelines developed by the China Council on Animal Care and the protocol approved by the Ren-Ji Hospital affiliated to Shanghai Jiao-Tong University School of Medicine.

**Gene Set Enrichment Analysis (GSEA).** GSEA is a method of analyzing and interpreting microarray and such data using biological knowledge,<sup>32</sup> and its application has been described previously.<sup>33</sup> The data in question is analyzed in terms of their differential enrichment in a predefined biological set of genes (representing pathways). These predefined biological sets can be published information about biochemical pathway or coexpression in a previous experiment. GSEA was performed using GSEA version 2.0 from the Broad Institute at MIT, MA, USA. Parameters used for the analysis were as follows. The gene expression data determined by Affymetrix HGU133A microarray were obtained from published literature via the GEO database (GSE41258). The 'C2' curated gene set were used for running GSEA and 1000 permutations were used to calculate *P*-value and permutation type was set to gene set. The maximum gene set size was fixed at 500 genes, and the minimum size fixed at 15 genes. The expression level of ELF3 was used as phenotype label, and 'Metric for ranking genes' was set to Pearson Correlation. All other basic and advanced fields were set to default.

**Statistical analysis.** Data from at least three independent experiments performed in triplicate are presented as the mean  $\pm$  S.D. Comparisons were performed using the Student's paired *t*-test, Spearman's correlation test or  $\chi^2$ -test; *P* < 0.05 was considered statistically significant.

### Conflict of Interest

The authors declare no conflict of interest.

**Acknowledgements.** This work was supported by grants from the National Natural Science Foundation of Key Program (No. 30830055), the Ministry of Public Health, China (No. 200802094), the Ministry of Education (No. 20090073110077) to JYF; and the Doctor Innovation Foundation of Shanghai Jiao-Tong University School Of Medicine (No. BXJ201219) to JLW; and the funded project of the Chinese National Natural Science Fund Committee (81201911) and the Research Project of Shanghai Science and Technology Commission (12ZR1446200) and the Research Project of Shanghai Science and Technology Commission (14QA1402700) to HMC.

- Ahn J, Sinha R, Pei Z, Dominianni C, Wu J, Shi J *et al*. Human gut microbiome and risk for colorectal cancer. *J Natl Cancer Inst* 2013; **105**: 1907–1911.
- Xu J, Wang J, Xu B, Ge H, Zhou X, Fang JY. Colorectal cancer cells refractory to anti-VEGF treatment are vulnerable to glycolytic blockade due to persistent impairment of mitochondria. *Mol Cancer Ther* 2013; **12**: 717–724.
- Jemal A, Bray F, Center MM, Ferlay J, Ward E, Forman D. Global cancer statistics. *CA Cancer J Clin*. 2011; **61**: 69–90.

- Ciznadija D, Tothill R, Waterman ML, Zhao L, Huynh D, Yu RM *et al*. Intestinal adenoma formation and MYC activation are regulated by cooperation between MYB and Wnt signaling. *Cell Death Differ* 2009; **16**: 1530–1538.
- Horst D, Chen J, Morikawa T, Ogino S, Kirchner T, Shivdasani RA. Differential WNT activity in colorectal cancer confers limited tumorigenic potential and is regulated by MAPK signaling. *Cancer Res* 2012; **72**: 1547–1556.
- Liu W, Liu Y, Guo T, Hu C, Luo H, Zhang L *et al*. TCF3, a novel positive regulator of osteogenesis, plays a crucial role in miR-17 modulating the diverse effect of canonical Wnt signaling in different microenvironments. *Cell Death Dis* 2013; **4**: e539.
- Hu X, Gao J, Liao Y, Tang S, Lu F. Retinoic acid alters the proliferation and survival of the epithelium and mesenchyme and suppresses Wnt/beta-catenin signaling in developing cleft palate. *Cell Death Dis* 2013; **4**: e898.
- Alexander MS, Kawahara G, Motohashi N, Casar JC, Eisenberg I, Myers JA *et al*. MicroRNA-199a is induced in dystrophic muscle and affects WNT signaling, cell proliferation, and myogenic differentiation. *Cell Death Differ* 2013; **20**: 1194–1208.
- Abu-Baker A, Laganieri J, Gaudet R, Rochefort D, Brais B, Neri C *et al*. Lithium chloride attenuates cell death in oropharyngeal muscular dystrophy by perturbing Wnt/beta-catenin pathway. *Cell Death Dis* 2013; **4**: e821.
- Cawthorn WP, Heyd F, Hegyi K, Sethi JK. Tumour necrosis factor-alpha inhibits adipogenesis via a beta-catenin/TCF4(TCF7L2)-dependent pathway. *Cell Death Differ* 2007; **14**: 1361–1373.
- Qiang YW, Hu B, Chen Y, Zhong Y, Shi B, Barlogie B *et al*. Bortezomib induces osteoblast differentiation via Wnt-independent activation of beta-catenin/TCF signaling. *Blood* 2009; **113**: 4319–4330.
- Lu Z, Hunter T. Wnt-independent beta-catenin transactivation in tumor development. *Cell cycle* 2004; **3**: 571–573.
- Yang W, Xia Y, Ji H, Zheng Y, Liang J, Huang W *et al*. Nuclear PKM2 regulates beta-catenin transactivation upon EGFR activation. *Nature* 2011; **480**: 118–122.
- Shatnawi A, Norris JD, Chaveroux C, Jasper JS, Sherk AB, McDonnell DP *et al*. ELF3 is a repressor of androgen receptor action in prostate cancer cells. *Oncogene* 2014; **33**: 862–871.
- Longoni N, Sarti M, Albino D, Civenni G, Malek A, Orтели E *et al*. ETS transcription factor ESE1/ELF3 orchestrates a positive feedback loop that constitutively activates NF-kappaB and drives prostate cancer progression. *Cancer Res* 2013; **73**: 4533–4547.
- Nakarai C, Osawa K, Matsubara N, Ikeuchi H, Yamano T, Okamura S *et al*. Significance of ELF3 mRNA expression for detection of lymph node metastases of colorectal cancer. *Anticancer Res* 2012; **32**: 3753–3758.
- Kaplan MH, Wang XP, Xu HP, Dosik MH. Partially unspliced and fully spliced ELF3 mRNA, including a new Alu element in human breast cancer. *Breast Cancer Res Treat* 2004; **83**: 171–187.
- Sheffer M, Bacolod MD, Zuk O, Giardina SF, Pincas H, Barany F *et al*. Association of survival and disease progression with chromosomal instability: a genomic exploration of colorectal cancer. *Proc Natl Acad Sci USA* 2009; **106**: 7131–7136.
- Mathiasen DP, Egebjerg C, Andersen SH, Rafn B, Puustinen P, Khanna A *et al*. Identification of a c-Jun N-terminal kinase-2-dependent signal amplification cascade that regulates c-Myc levels in ras transformation. *Oncogene* 2012; **31**: 390–401.
- Haupt S, Gamell C, Wolyniec K, Haupt Y. Interplay between p53 and VEGF: how to prevent the guardian from becoming a villain. *Cell Death Differ* 2013; **20**: 852–854.
- Fahang Ghahremani M, Goossens S, Nittner D, Bisteau X, Bartunkova S, Zwolinska A *et al*. p53 promotes VEGF expression and angiogenesis in the absence of an intact p21-Rb pathway. *Cell Death Differ* 2013; **20**: 888–897.
- Shan L, Li X, Liu L, Ding X, Wang Q, Zheng Y *et al*. GATA3 cooperates with PARP1 to regulate CCND1 transcription through modulating histone H1 incorporation. *Oncogene* 2013; e-pub ahead of print 15 July 2013; doi:10.1038/onc.2013.270.
- Voloshanenko O, Erdmann G, Dubash TD, Augustin I, Metzgi M, Moffa G *et al*. Wnt secretion is required to maintain high levels of Wnt activity in colon cancer cells. *Nat Commun* 2013; **4**: 2610.
- Bandapalli OR, Dihlmann S, Helwa R, Macher-Goeppinger S, Weitz J, Schirmacher P *et al*. Transcriptional activation of the beta-catenin gene at the invasion front of colorectal liver metastases. *J Pathol* 2009; **218**: 370–379.
- Liu G, Jiang S, Wang C, Jiang W, Liu Z, Liu C *et al*. Zinc finger transcription factor 191, directly binding to beta-catenin promoter, promotes cell proliferation of hepatocellular carcinoma. *Hepatology* 2012; **55**: 1830–1839.
- Otero M, Plumb DA, Tsuchimochi K, Dragomir CL, Hashimoto K, Peng H *et al*. E74-like factor 3 (ELF3) impacts on matrix metalloproteinase 13 (MMP13) transcriptional control in articular chondrocytes under proinflammatory stress. *J Biol Chem* 2012; **287**: 3559–3572.
- Kushwah R, Oliver JR, Wu J, Chang Z, Hu J. Elf3 regulates allergic airway inflammation by controlling dendritic cell-driven T cell differentiation. *J Immunol* 2011; **187**: 4639–4653.
- Kong X, Qian J, Chen LS, Wang YC, Wang JL, Chen H *et al*. Synbindin in extracellular signal-regulated protein kinase spatial regulation and gastric cancer aggressiveness. *J Natl Cancer Inst* 2013; **105**: 1738–1749.

29. Xu J, Wang J, Hu Y, Qian J, Xu B, Chen H *et al*. Unequal prognostic potentials of p53 gain-of-function mutations in human cancers associate with drug-metabolizing activity. *Cell Death Dis* 2014; **5**: e1108.
30. Xu J, Reumers J, Couceiro JR, De Smet F, Gallardo R, Rudyak S *et al*. Gain of function of mutant p53 by coaggregation with multiple tumor suppressors. *Nat Chem Biol* 2011; **7**: 285–295.
31. Xu J, Zhou X, Wang J, Li Z, Kong X, Qian J *et al*. RhoGAPs attenuate cell proliferation by direct interaction with p53 tetramerization domain. *Cell Rep* 2013; **3**: 1526–1538.
32. Subramanian A, Kuehn H, Gould J, Tamayo P, Mesirov JP. GSEA-P: a desktop application for Gene Set Enrichment Analysis. *Bioinformatics* 2007; **23**: 3251–3253.
33. Xu J, Qian J, Hu Y, Wang J, Zhou X, Chen H *et al*. Heterogeneity of Li-Fraumeni Syndrome links to unequal gain-of-function effects of p53 mutations. *Sci Rep* 2014; **4**: 4223.



**Cell Death and Disease** is an open-access journal published by *Nature Publishing Group*. This work is licensed under a Creative Commons Attribution-NonCommercial-NoDerivs 3.0 Unported License. The images or other third party material in this article are included in the article's Creative Commons license, unless indicated otherwise in the credit line; if the material is not included under the Creative Commons license, users will need to obtain permission from the license holder to reproduce the material. To view a copy of this license, visit <http://creativecommons.org/licenses/by-nc-nd/3.0/>

Supplementary Information accompanies the paper on Cell Death and Disease website (<http://www.nature.com/cddis>)